Article

An Evaluation of Correlations for Predicting the Heat Transfer Coefficient during the Condensation of Saturated and Superheated Vapors Inside Channels

Mirza M. Shah

Engineering Research Associates, 10 Dahlia Lane, Redding, CT 06896, USA; mshah.erc@gmail.com;
Tel.: +1-860-869-1328

Abstract: Condensation heat transfer is involved in many industrial applications. Therefore, it is important to know the relative accuracy of the available methods for predicting heat transfer. Condensation can occur with saturated as well as superheated vapors. Predictive methods for both conditions were evaluated using a wide range of data. Twelve well-known correlations for the condensation of saturated vapor, including the most recent ones, were compared with data for 51 pure fluids and mixtures from 132 sources in horizontal and vertical channels of many shapes. Channel hydraulic diameters were 0.08–49 mm, the mass flux was 1.1–1400 kg/m^{2}s, and the reduced pressure range was 0.0006–0.949. The fluids included water, CO_2, ammonia, hydrocarbons, halocarbon refrigerants, various chemicals, and heat transfer fluids. The best predictive technique was identified. The three most commonly used models for heat transfer during the condensation of superheated vapors were studied. They were first compared with test data using measured saturated condensation and forced convection heat transfer coefficients to select the best model. The selected model was then compared with test data using various correlations for heat transfer coefficients needed in the model. The best correlations to use in the model were identified. The results of this research are presented, as are recommendations for use in design.

Keywords: condensation; heat transfer; saturated vapors; superheated vapors; inside channels; correlations

1. Introduction

Condensation in channels occurs in many applications, including refrigeration, power generation, and chemical processing. Condensation occurs when the wall temperature is lower than the saturation temperature of the vapor from saturated as well as superheated vapors. Methods for the accurate prediction of heat transfer during the condensation of saturated and superheated vapors are needed to ensure the correct sizing of the condensers. Numerous correlations have been proposed for the condensation of saturated vapors. The best-known among them were recently evaluated in a paper by the author by comparing them with data for 51 pure fluids and mixtures from 132 sources in horizontal and vertical channels of many shapes. The channel hydraulic diameters were 0.08–49 mm, the mass flux was 1.1–1400 kg/m^{2}s, and the reduced pressures range was 0.0006–0.949. The fluids included water, CO_2, ammonia, hydrocarbons, halocarbon refrigerants, various chemicals, and heat transfer fluids. Some new correlations verified with wide ranges of data have recently been published; they are said to be more accurate than other correlations. Therefore, it is desirable to also evaluate their accuracy along with the other correlations. This has been investigated in the present paper, and its results are presented in this paper. Several methods have been proposed for the calculation of heat transfer during the condensation of superheated vapors, but none of them have been adequately evaluated. A preliminary study by Shah (2023) [1] focused on some of them. In the present study, three of the most commonly used models were evaluated by comparing them with a wide range of test data. It was found that one of those models is considerably superior to the other two. That model was then compared with test data using various correlations for

saturated condensation and forced convection heat transfer in order to identify the ones that give the best agreement.

The following paper reviews the previous work on this topic, and the results of the present study are presented. Recommendations are made regarding the application of the results to the design of condensers.

Please note that this paper is concerned only with film condensation in commercially manufactured channels. Dropwise condensation and enhanced surfaces are not within the scope of this paper.

2. Previous Work

2.1. Condensation of Saturated Vapors

A large number of experimental studies have been conducted on heat transfer during condensation in mini and macro channels of various shapes and types. These have been reviewed and listed in Shah (2021) [2], Shah (2022) [3], Nie et al. (2023) [4], and Marinheiro et al. (2023) [5].

Many correlations have been published, including those by the present author. The first study, by Shah (1979) [6], continues to be widely used, but it is limited to lower pressures and higher flow rates. Several improved versions have been published. Subsequent correlations in Shah (2009, 2013) [7,8] were shown to be applicable at pressures close to the critical pressures and for flow rates ranging from very low to very high. The Shah (2016) [9] correlation took into account the effects of surface tension, making it applicable to both mini and macro channels. Further improvements were made in several papers. The final version is Shah (2022) [10] which differs from that in Shah (2022) [3] only for quality ≥ 0.99. Among other correlations that have agreed with a wide range of test data are Cavallini et al. (2006) [11], Dorao and Fernandini (2018) [12], Hosseini et al. (2020) [13], and Moradkhani et al. (2022) [14]. The aforementioned correlations are intended for both mini and macro channels. A number of correlations have been published, specifically for mini-channels. The most verified among them is the correlation given by Kim and Mudawar (2013) [15]. In Shah (2022) [3], it was shown that the Shah correlation was considerably more accurate than the other correlations, especially when $We_{GT} < 100$; this is the range in which the surface tension effect becomes important. Most recently, Nie et al. (2023) [4] and Marinheiro et al. (2023) [5] presented correlations that were shown to align well with wide-ranging databases and were stated to be more accurate than other correlations. Therefore, it is desirable to also evaluate these new correlations to determine their merits compared with the other correlations. This has been conducted in the present research.

The correlation found in the work of Nie et al. (2023) [4] was obtained through the use of machine learning, and it is based entirely on data for horizontal tubes. It is as follows:

For annular flow,

$$h_{an} = 0.038 Re_{LS}^{0.72} Pr_L^{0.27} \left(\frac{\mu_L}{\mu_G} \right)^{0.84} \left(\frac{\rho_G}{\rho_L} \right)^{0.37} \frac{\varphi_G}{X_{tt}} \frac{k_L}{D} \tag{1}$$

For non-annular flow,

$$h_{nan} = h_{an} + 0.012 Re_{LS}^{0.85} \left(\frac{x}{1-x} \right)^{1.1} \left(\frac{\rho_G}{\rho_L} \right)^{-0.55} \left(\frac{\rho_L - \rho_G}{Fr_{GS}\rho_G} \right)^{0.55} \frac{k_L}{D} \tag{2}$$

where

$$Fr_{GS} = \frac{(Gx)^2}{\rho_G^2 g D} \tag{3}$$

$$\varphi_G = X_{tt}^{0.2} + 0.83 \left(\frac{x}{J_G} \right)^{0.84} X_{tt}^{1.2} \tag{4}$$

$$J_g = \frac{xG}{(gD\rho_G(\rho_L - \rho_G))^{0.5}} \tag{5}$$

The identification of the flow pattern is carried out as follows. Annular flow occurs when

$$J_g \geq 2.5 \text{ and } G > G_w \tag{6}$$

Otherwise, the flow is non-annular. G_w is defined as follows:

$$G_w = \rho_L (gD)^{0.5} \left(0.54 - \frac{0.96}{Bd^2} - \frac{4.2}{Bd} \right) \tag{7}$$

Bd is the Bond number, which is defined as follows:

$$Bd = g(\rho_L - \rho_G)D^2 \, \sigma^{-1} \tag{8}$$

The correlation of Marinheiro et al. (2023) [5] was based on data relating to both horizontal and vertical channels, round as well as non-circular. The data included pure fluids as well as mixtures. It is given in the following equation.

$$h_{TP} = 0.055 Re_{TP}^{0.732} Pr_{TP}^{0.269} Fr_{LT}^{-0.091} \frac{k_L}{D} \tag{9}$$

$$Re_{TP} = Re_{LS} + Re_{GS} \tag{10}$$

Re_{LS} and Re_{GS} represent the superficial Reynolds numbers of the liquid and vapor phases, respectively.

$$Pr_{TP} = Pr_L + Pr_G \tag{11}$$

For non-circular channels, the hydraulic diameter is used in this correlation. For mixtures, they found that the use of Bell and Ghaly [16] correction for mass transfer effects deteriorated the agreement with the data. Hence, their correlation is to be used without correction for the effects of mass transfer.

2.2. Superheated Vapors

Various models for superheated condensation were reviewed by Shah (2023). Some of the text below is taken from this review.

McAdams (1954) [17] studied the data of several researchers for mean heat transfer during the complete condensation of superheated vapors. These studies showed that the total heat transfer with superheated vapors was only slightly higher than with saturated vapors. For example, Merkel (1927) [18] found that for 82 K superheated steam, heat flux was only 3% higher than with saturated steam. Therefore, McAdams recommended that calculations can be carried out while neglecting the effect of superheating without significant error. Thus, the mean heat flux qm for the condenser is given as follows:

$$q_m = h_{SAT,m}(T_{SAT} - T_{w,m}) \tag{12}$$

where $T_{w,m}$ is the mean wall temperature of the condenser.

Altman et al. (1959) [19] performed tests with R-22 superheated up to 23 K. They concluded that the change in the heat transfer coefficient is not related to the extent of superheating but is related to ΔTSAT. They only reported the mean heat transfer coefficient, and sufficient details have not been provided for their analysis.

Miropoloskiy et al. (1974) [20] performed tests for the condensation of saturated and superheated steam in tubes. The pressure varied from 4 to 180 bar. They provided a graphical correlation that agrees with their own data. They did not compare it to any other data. The data shown in the figures in their paper lack the information needed for comparison with other correlations.

Lee et al. (1991) [21] condensed R-22 in a horizontal tube. Superheating was undertaken to 65 K, and the pressure ranged from 7.64 to 13.55 bar. They found that their saturated condensation data were in good agreement with the Shah (1979) [6] correlation. For the condensation of superheated vapor, they proposed that superheated vapor loses

heat to the condensate layer via forced convection heat transfer, and the condensate transfers heat to the coolant through the wall in the same way as in the condensation of saturated vapor. Accordingly, they gave the following relation for the local heat transfer coefficient.

$$h_{TP}(T_G - T_w) = h_{SAT}(T_{SAT} - T_w) + h_{FC}(T_G - T_{SAT}) \tag{13}$$

The forced convection heat transfer coefficient of the superheated vapor was calculated using the Gnielinski (1976) [22] formula, while the condensing heat transfer coefficient h_{SAT} was calculated using the Shah (1979) [6] correlation. The area for the heat transfer between the vapor and condensate was calculated, taking into consideration the thickness of the liquid film, which was estimated based on the calculated void fraction. Good agreement with their own data was reported.

Webb (1998) [23] argued that heat transfer from the superheated vapor to the condensate film involves mass transfer, which causes bulk convection in the superheated vapor, thus enhancing heat transfer. He modified Equation (13) to take into account this enhancement to the following form.

$$h_{TP}(T_{SAT} - T_w) = h_{SAT}(T_{SAT} - T_w) + (h_{FC} + q_{lat}C_{PG}/i_{LG})(T_G - T_{SAT}) \tag{14}$$

Webb states that this equation is applicable to all types of condensers, condensation inside channels or on their external surfaces. He only compared Equation (14) to the data of Lee et al. (1991) [21] mentioned above and reported good agreement. hSAT was calculated using the Shah (1979) [6] correlation.

Longo et al. (2015) [24] incorporated the Webb model into their procedure for calculating the mean heat transfer coefficient for plate-type heat exchangers. They reported good agreement with the mean heat transfer coefficients for the complete condensation of several fluids.

Karwacki et al. (2011) [25] visually observed the condensation of superheated isobutane and R-507 in an air-cooled tube. They observed a thin liquid film around the tube which was mixed with oil. They also performed heat transfer tests but have not provided any heat transfer data.

Kondou and Hrnjak (2012) [26] performed tests in a horizontal 6.1 mm tube with CO_2 and R-410A at high pressures up to near-critical levels. To analyze their data, they adopted the model of Equation (13), but they neglected the thickness of the condensate film. They used a modified form of the Cavallini et al. (2006) [11] correlation to calculate h_{SAT}. For h_{FC}, they used the Gnielinski (1976) [11] correlation with wall temperature correction carried out using Pethukov (1970) [27]. The correlation is shown below.

$$f = \lfloor 1.82 log_{10} Re_{GT} - 1.64 \rfloor^{-2} \tag{15}$$

$$h_{FC} = F_a[(k_G/D)(f/8)(Re_{GT} - 1000)Pr_G]/\left[1 + 12.7(f/8)^{0.5}\left(Pr_G^{2/3} - 1\right)\right] \tag{16}$$

$$F_a = (T_w/T_G)^{-0.36} \tag{17}$$

F_a is the correction factor, according to Pethukov (1970) [27]. All of the fluid properties are at the bulk vapor temperature. They reported good agreement with their own data.

Agarwal and Hrnjak (2014, 2015) [28,29] measured heat transfer coefficients during the condensation of superheated R-134a, R-32, and R-1234ze in a 6.1 mm horizontal tube. They compared their data with Equation (13). h_{SAT} was calculated using the Cavallini et al. (2006) [11] correlation, and h_{FC} was calculated using the Gnielinski correlation, as given in Equations (15) and (16). Condensate film thickness was taken into consideration when calculating the heat transfer between the vapor and the condensate film. A good agreement was found with their own data.

Xiao and Hrnjak (2016) [30] performed tests with superheated R-134a condensing in a 6.1 mm diameter horizontal tube with a mass flux of 50 to 200 kg/m^{2}s.

Xiao and Hrnjak (2017) [31] presented a model for saturated, superheated, and subcooled condensation based on non-equilibrium throughout the condensation process. It

uses a film heat transfer coefficient based on the temperature at the interface between the liquid and the vapor. It involves the calculation of the flow pattern using the Xiao and Hrnjak (2015) [32] map and void fraction by their own correlation. This model was reported to be in good agreement with the data of Kondou and Hrnjak (2012) [26] and Agarwal and Hrnjak (2014, 2015) [28,29], as well as their own data. Good agreement over the entire range is reported, but the results for the saturated and superheated regions are not given separately. All these data were obtained using a 6.1 mm horizontal tube.

Sierres et al. (2017) [33] tested condensation in a vertical tube using superheated R-134a and R-437. Only the average heat transfer coefficients for complete condensation have been reported.

Jacob and Fronk (2021) [34] performed tests on five zeotropic mixtures of halocarbon refrigerants in a 4.7 mm diameter horizontal tube. The tests included superheated and saturated condensation. They proposed a new model specifically for mixtures, which was in good agreement with their own data. Their model essentially uses Equation (13) together with the Bell and Ghaly correction for mass transfer. Gnielinski correlation is used for h_{FC}, and Cavallini et al. correlation is used for h_{SAT}. The thickness of the condensate film is considered negligible. They compared their data with the models of Kondou and Hrnjak (2012) [26], Agarwal and Hrnjak (2014) [28], and Xiao and Hrnjak (2017) [31], as described above. To correct for mass transfer effects, Bell and Ghaly correction was applied. All three models were found to be satisfactory in the superheated region. In the saturated region, the models of Xioa and Hrnjak and Agarwal and Hrnjak yielded large deviations, while the Kondou and Hrnjak model was satisfactory.

All of the above-mentioned experimental studies were carried out using plain tubes. Kondou and Hrnjak (2012) [35] performed tests on the condensation of superheated CO_2 in two types of internally finned tubes. The data were correlated using Equation (13) with h_{SAT} and h_{FC} calculated with correlations suitable for such tubes. A satisfactory agreement was found.

3. Data Analysis

3.1. Saturated Vapor Condensation

A very wide-ranging database was available, as described in Shah (2022a, 2022b) [3,10]. The range of data in the database is given in Table 1. It can be seen that it has 51 fluids (pure and mixtures), horizontal and vertical flow, various channel types (annuli, round tubes, channels of various shapes such as rectangular, triangular, etc.), hydraulic diameters from 0.08 to 49 mm, reduced pressures from very low to near critical, and flow rates from very low to very high. The fluids include water, chemicals, halocarbon refrigerants, cryogens, carbon dioxide, and ammonia; thus, an extremely wide range of properties is included.

Table 1. Range of data for condensation of saturated vapors that were analyzed. This was modified from Shah (2022a) [3] to include the data analyzed in Shah (2022b) [10].

Parameter	Data Range
Fluids	Water, R-11, R-12, R-22, R-32, R-41, R-113, R-123, R-125, R-134a, R-141b, R-142b, R-152a, R-161, R-236ea, R-245fa, R-404A, R-410A, R-448A, R-449A, R-450A, R-502, R-507, R-513A, R-452B, R-454C, R-455A, R-1234fa, R-1234yf, R-1234ze(E), DME, butane, propane, carbon dioxide, methane, FC-72, isobutane, propylene, benzene, ethanol, methanol, toluene, Dowtherm 209, HFE-7000, HFE-7100, ethane, pentane, Novec 649, ammonia, and nitrogen (51 fluids)
Geometry	Round, square, rectangle, semi-circle, triangle, and barrel-shaped single and multi channels. All sides cooled or one side insulated. Cooled partly or on all sides. Annuli.
Orientation	Horizontal, vertical down
Aspect ratio, width/height	0.14 to 2.0
D_{HYD}, mm	0.08 to 49.0
Reduced pressure	0.0006 to *0.949*

Table 1. *Cont.*

Parameter	Data Range
G, kg m^{-2} s^{-1}	1.1 to 1400
x, %	0.01 to 1.0
We$_{GT}$	0.15 to 79,060
Fr$_{LT}$ for horizontal channels	*7.7 × 10^{-6}* to 4070
Glide of mixtures, K	0.1 to 9.5
Bond number	0.033 to 2392
Number of data sources	132 (112 Horizontal, 16 vertical down, and 4 both)
Number of data sets	267 (238 horizontal and 29 vertical down)

These data were compared to all the correlations that were evaluated in Shah (2022a, 2022b) [3,10] in addition to the new correlations of Nie et al. (2023) [4] and Marinheiro (2023) [5], which have been described in Section 2.1.

In calculations with all Shah correlations, D$_{HP}$ was used to calculate the single-phase heat transfer coefficient and the Reynolds number. The same was also carried out with other correlations, except for those of Kim and Mudawar (2013) [15], Dorao and Fernandino (2018) [12], Hosseini et al. (2020) [13], Moradkhani et al. (2021) [14], and Marinheiro et al. (2023) [5]. For these correlations, D$_{HYD}$ was used as the equivalent diameter in all calculations because that was specified by these authors. Nie et al. (2023) [4] did not specify the equivalent diameter to be used; D$_{HYD}$ was also used in the calculations.

Where the authors reported mean heat transfer coefficient data, they were analyzed using arithmetic mean quality.

The properties of HFE-7100 and FC-72 were obtained from their manufacturer, the 3M Corporation. The properties of Dowtherm 209 were taken from Blangetti and Schlunder (1979) [36]. The surface tension of HFE-7000 was taken from Vins et al. (2021) [37]. All of the other properties were obtained from REFPROP 9.1, Lemmon et al. (2013) [38]. All of the properties used were at saturation temperature. The deviations in the correlations were calculated as below.

Mean absolute deviation (MAD) is defined as follows:

$$MAD = \frac{1}{N}\sum_{1}^{N} ABS\left\{ \left(h_{predicted} - h_{measured} \right) / h_{measured} \right\}$$ (18)

Average deviation (AD) is defined as follows:

$$AD = \frac{1}{N}\sum_{1}^{N} \left\{ \left(h_{predicted} - h_{measured} \right) / h_{measured} \right\}$$ (19)

Tables 2 and 3 give the deviations of various correlations for various conditions. For all data, the Shah (2022b) [10] correlation has the least MAD of 17.7%. The next best is the Shah (2009, 2013) [7,8] correlation, with a MAD of 20.3%. Details of the results are discussed in Section 4.

Table 2. Deviations of various correlations with data for saturated vapors; effect of orientation, tube diameter, and Weber number.

Orientation	Dia. mm	We$_{GT}$	N	Deviation, %, MAD (Upper Row), AD (Lower Row)											
				Kim and Mudawar	Ananiev et al.	Dorao and Fernandino	Hosseini et al.	Moradkhani et al.	Moser et al.	Traviss et al.	Akers et al.	Marinheiro et al.	Nie et al.	Shah (2009,2013) [7,8]	Shah (2022b) [10]
Horizontal	≤3	<100	788	29.5 / −17.5	40.6 / −37.2	35.0 / −31.8	39.4 / −29.8	27.2 / −16.3	31.8 / −5.1	43.0 / 9.8	150.6 / 150.3	28.6 / −23.6	74.3 / 56.1	31.9 / −24.1	20.4 / −2.0
	≤3	>100	2033	19.4 / −8.5	19.7 / −8.2	19.8 / −7.4	22.3 / −3.5	20.8 / −6.7	34.1 / 26.3	99.4 / 95.8	105.4 / 103.8	21.0 / −11.6	40.7 / 26.7	21.3 / 6.7	18.5 / −1.9
	≤3	All	2821	22.3 / −11.4	25.8 / −16.5	26.3 / −16.7	27.3 / −11.4	22.9 / −19.9	33.3 / 17.5	88.1 / 17.8	116.3 / 114.9	23.2 / −14.8	50.1 / 34.9	24.2 / −1.9	19.0 / −1.9
	>3	<100	255	65.0 / 8.6	56.4 / −56.4	38.4 / −13.2	47.4 / 5.4	38.3 / −29.5	43.8 / −41.6	43.5 / −10.7	36.2 / −0.2	40.6 / −33.6	83.4 / 77.4	29.0 / −9.6	26.1 / 6.2
	>3	>100	4606	27.1 / −21.1	23.9 / −13.5	18.7 / 0.9	28.2 / 4.8	17.4 / −2.4	34.4 / 17.1	118.3 / 113.3	26.8 / −4.2	18.3 / −10.3	42.4 / 23.8	17.8 / 3.3	16.5 / 0.6
	>3	All	4861	29.0 / −19.6	25.6 / −15.8	19.7 / 0.1	28.4 / −1.8	18.6 / −4.2	34.8 / 16.3	113.4 / 106.7	27.6 / −2.2	19.5 / −11.5	44.6 / 26.7	18.4 / 2.6	17.0 / 0.9
	All	<100	1043	38.3 / −12.2	45.2 / −42.5	35.9 / −27.2	42.0 / −22.6	30.9 / −20.9	35.4 / −14.0	41.3 / 8.7	124.0 / 115.2	31.6 / −25.6	76.5 / 61.3	31.1 / −10.5	21.8 / −0.1
	All	>100	6639	24.7 / −17.3	22.6 / −11.9	18.9 / −1.1	26.3 / 1.5	18.5 / −4.0	34.3 / 21.9	111.8 / 107.3	51.1 / 30.1	19.1 / −10.7	41.9 / 24.7	18.9 / 4.3	17.1 / −0.2
	All	All	7682	26.6 / −12.6	25.7 / −16.1	21.2 / −4.7	29.1 / −1.1	20.2 / −6.3	34.0 / 16.9	102.3 / 93.9	61.0 / 41.7	20.8 / −12.7	46.6 / 29.7	20.6 / 1.0	17.8 / −0.2
Vertical Downflow	≤3	All	272	23.7 / −8.2	28.6 / −21.8	25.4 / −19.1	32.9 / −14.8	19.6 / 2.4	31.3 / 6.6	69.4 / 66.2	128.0 / 128.0	23.1 / −5.8	36.4 / 18.9	20.7 / −5.9	20.7 / −5.9
	>3	All	538	40.2 / 14.1	33.8 / −1.5	38.8 / −35.4	40.5 / 15.0	31.1 / 6.4	33.2 / 6.4	60.1 / 39.0	42.7 / 4.6	32.9 / −9.9	179.5 / 179.1	15.8 / 1.9	15.8 / 1.9
	All	All	810	34.7 / 6.6	32.1 / −8.3	34.3 / −29.9	37.9 / 5.0	27.2 / 3.4	32.5 / 6.5	63.2 / 48.1	71.3 / 46.0	29.6 / −8.6	131.5 / 121.3	17.4 / −0.7	17.4 / −0.7
Horizontal and Vertical	All	<100	1271	42.4 / −6.3	44.9 / −42.3	35.3 / −24.2	43.6 / −21.0	31.2 / −21.3	35.7 / −15.4	42.9 / 10.5	121.1 / 108.9	32,3 / −24.6	82.6 / 68.7	29.3 / −8.3	21.6 / −1.6
	All	>100	7221	24.7 / −15.8	23.0 / −10.6	19.6 / −0.6	26.8 / 2.4	19.1 / −2.8	33.9 / 21.6	108.3 / 103.7	51.9 / 30.8	19.8 / −10.2	49.8 / 33.5	18.7 / 4.2	17.0 / 0.0
	All	All	8492	27.3 / −14.4	26.3 / −15.3	21.9 / −4.1	29.3 / −1.1	20.9 / −5.4	34.2 / 16.1	98.5 / 89.5	62.0 / 42.1	21.7 / −12.3	54.7 / 38.8	20.3 / 0.8	17.7 / −0.2

Table 3. Deviation of correlations with the data for saturated condensation of various types of fluids.

Fluid	Number of Sources	N	Deviation, %, MAD (Upper Row), AD (Lower Row)											
			Kim and Mudawar	Ananiev et al.	Dorao and Fernandino	Hosseini et al.	Moradkhani et al.	Moser et al.	Traviss et al.	Akers et al.	Marinheiro et al.	Nie et al.	Shah (2013) [8]	Shah (2022b) [10]
Water	14	333	38.7 4.0	49.3 7.2	32.6 −24.0	43.3 −3.8	37.3 −13.3	36.0 −26.9	84.8 57.1	34.8 −16.2	48.5 −48.1	146.8 146.7	17.8 −2.0	15.9 3.4
Carbon dioxide	9	386	31.7 −10.4	29.8 −8.0	23.3 7.1	29.4 −6.0	24.3 −6.8	49.5 29.0	164.4 157.8	43.1 36.1	19.3 −7.1	34.7 6.4	22.9 7.8	20.9 2.8
Hydrocarbons	24	1536	21.9 −11.3	19.0 0.0	22.1 10.5	15.5 −7.0	16.2 −5.1	45.2 41.1	151.8 150.8	49.2 25.3	18.4 −18.9	45.9 30.8	19.4 12.5	17.2 9.1
Ammonia	1	79	32.6 −27.3	41.4 −38.3	44.7 −41.1	54.4 −54.1	24.3 −16.2	46.9 −45.2	29.0 8.5	54.3 52.8	42.8 −32.8	27.3 16.7	39.7 −35.7	34.2 −24.2
Halocarbon refrigerants	112	5734	28.0 −6.6	26.2 −19.8	20.1 −6.8	31.5 2.7	20.6 −4.7	29.6 11.9	85.5 75.9	67.3 48.7	20.7 −11.2	46.7 30.0	20.3 −1.4	17.5 −2.7
HFEs, FC-72, Dowtherm	6	191	21.9 −12.9	25.8 −13.0	40.3 4.6	38.3 −10.3	36.6 −3.3	57.4 46.2	51.7 2.0.0	91.7 81.3	25.4 −5.4	275.3 275.3	21.8 −8.5	20.9 3.0

3.2. Superheated Vapor Condensation

3.2.1. Evaluation of Models

Models Evaluated

The various models that have been proposed for superheated condensation are discussed in Section 2.2. The ones selected for evaluation are discussed below.

The model proposed by McAdams, Equation (12), has been widely used due to its simplicity. It neglects the effect of superheating on condensation heat transfer. It is named Model 1. In terms of the local heat flux q, it is as below

$$q = h_{SAT}(T_{SAT} - T_w) \tag{20}$$

Jacob and Fronk (2021) [34] found the models of Xiao and Hrnjak and Agarwal and Hrnjak to be very inaccurate in the saturated condensation region. While designing a condenser, it is desirable to use the same formula for h_{SAT} in the superheated region as in the saturated region. Hence, these two models are not considered for evaluation. The models of Lee et al., Kondu and Hrnjak, and Jacob and Fronk all use Equation (13), the differences being in some details of the calculation method. Hence, this is one of the models to be evaluated. It is called Model 2. In terms of local heat flux q, it is written as follows:

$$q = h_{SAT}(T_{SAT} - T_w) + h_{FC}(T_G - T_{SAT}) \tag{21}$$

The Webb model represented by Equation (14) is called Model 3. The local heat flux q is written as follows:

$$q = h_{SAT}(T_{SAT} - T_w) + (h_{FC} + q_{lat}C_{PG}/i_{LG})(T_G - T_{SAT}) \tag{22}$$

q_{lat} is the heat flux due to phase change alone

Comparison of Models Using Measured h_{SAT} and h_{FC}

The predictions of the models described in this Section will vary with the correlations used to calculate h_{SAT} and h_{FC}. To ensure the correct evaluation of the accuracy of the models, the measured values of h_{SAT} and h_{FC} were used. All of the data listed in Table 4 provide measured h_{SAT} at x = 1. Most of the data from the work of Hrnjak and coworkers provide measured h_{FC}, and in such cases, they show close agreement with the correlation of Gnielinski described in Section 2. Hence, in the few cases where it was not given in their data figures, h_{FC} was calculated using the Gnielinski correlation. The data of Lee et al. (1991) [21] gave neither h_{SAT} nor h_{FC}. Hence, it was not included in this comparison.

Table 4. Deviations of various models for the condensation of superheated vapors in tubes using measured forced convection and condensing heat transfer coefficients. All tubes were horizontal.

Source	Tube Type	Dia., mm	Fluid	Reduced Pressure	G Kg/m²s	q kW/m²	Superheat K	Re$_{GT}$ X 10^{-3}	N	Deviation, %, MAD (Upper Row)/AD (Lower Row)		
										Model 1	Model 2	Model 3
Fujii et al. (1978) [39]	Plain	21.4	R-113	0.0252 0.0323	45 115	10 11	2.2 41.5	77 211	15	43.9 −43.9	17.2 −17.2	15.1 −9.9
Kondou and Hrnjak (2011, 2012a, 2012b) [26,35,40]	Plain	6.1	CO$_2$	0.678 0.9492	100 150	10	0.5 16.9	33 51	7	32.9 −26.5	17.9 −1.1	33.3 23.1
Kondou and Hrnjak (2012a) [26]	Plain	6.1	R-410A	0.5493 0.9468	100 200	10 20	0.2 36.0	30 79	35	25.6 −23.1	13.7 5.5	47.4 42.2
Agarwal and Hrnjak (2015) [29]	Plain	6.1	R-134a	0.3247	100	10	0 19.3	44 47	4	14.7 −14.7	16.4 12.1	22.6 18.2
			R-1234ze	0.2743	100	10	1.7 41.8	39 45	5	30.7 −28.5	18.6 18.6	27.3 27.3
			R-32	0.5433	100	10	0.9 25.2	39 41	6	35.3 −35.3	17.6 10.0	26.0 18.7

Table 4. *Cont.*

Source	Tube Type	Dia., mm	Fluid	Reduced Pressure	G Kg/m²s	q kW/m²	Superheat K	Re_GT X 10⁻³	N	Deviation, %, MAD (Upper Row)/AD (Lower Row)		
										Model 1	Model 2	Model 3
Kondou and Hrnjak (2012b) [35]	Finned, Type A	6.1	CO₂	0.8137	100	10	0.3 6.2	32 34	4	31.8 −31.8	14.2 −13.3	14.1 −5.2
	Finned, Type B			0.8137	100	10	0.1 3.8	32 34	2	14.5 −14.5	3.6 3.6	9.1 9.1
All sources	Plain, Finned	5.1 21.4		0.0252 0.9492	45 200	10 20	0 41.8	30 211	109	30.9 −27.9	15.9 0.6	33.4 23.9

Calculations with Model 3 require q_{lat} the heat flux due to phase change, while the test data provide the total heat flux, which also includes the heat flux due to condensation. q_{lat} is calculated using the following equation.

$$q_{lat} = h_{SAT}(T_{SAT} - T_w) \qquad (23)$$

The deviations of each data set are listed in Table 4. These are defined as below. MAD (mean absolute deviation) is defined as follows:

$$MAD = \frac{1}{N}\sum_1^N ABS\left\{\left(q_{predicted} - q_{measured}\right)/q_{measured}\right\} \qquad (24)$$

The average deviation (AD) is defined as follows:

$$AD = \frac{1}{N}\sum_1^N \left\{\left(q_{predicted} - q_{measured}\right)/q_{measured}\right\} \qquad (25)$$

It can be seen that Model 2 is by far the most accurate, its MAD (mean absolute deviation) being 15.9%, and those of Model 1 and Model 3 are 30.9% and 33.4%, respectively. Model 1 always underpredicts. Model 3, which was proposed by Webb (1998) [23], overpredicts most data, with its AD being +23.9%.

Model 2 is clearly the best and was chosen for further evaluation.

Evaluation of Model 2 Using Various Correlations

As shown in this Section, Model 2 was found to be the most accurate model. This conclusion was reached using measured h_{SAT} and, in most cases, using the measured values of h_{FC}. It is now desired to know which correlations for h_{SAT} and h_{FC} give the best performance when using Model 2. This evaluation is limited to plain tubes.

For h_{FC}, two correlations were tried. One was the correlation of Gnielinski (1976) [22] with the correction by Pethukov (1970) [27], as given by Equations (15)–(17). The other was the correlation of Dittus and Boelter (1930) [41], which is given by the following formula.

$$h_{FC} = 0.023 Re_{GT}^{0.8} Pr_G^{0.4} k_G / D \qquad (26)$$

All properties were calculated at the bulk temperature of the vapor. The two correlations were tried together with the various correlations for h_{SAT}, which were tried. The deviations using the Gnielinski correlations and the Dittus–Boelter correlation were very close to each other. All of the results reported were obtained through the use of Gnielinski correlation, as shown in Equations (15)–(17).

For the condensation of saturated vapors, the most verified correlation is that of Shah (2022b) [10], as shown in Section 3.1. According to this correlation, surface tension has an effect when $We_{GT} < 100$. It is defined as follows:

$$We_{GT} = \frac{G^2 D}{\rho_G \sigma} \qquad (27)$$

Considering mini-channels to be those affected by surface tension, channels with $We_{GT} < 100$ are mini-channels, and those with $We_{GT} > 100$ are macro or conventional channels. While Shah (2022b) [10] was found to give the least MAD for both macro and mini channels, other correlations that had a reasonable agreement with macro channel data were those of Moradkhani et al. (2021) [14], Dorao and Fernandino (2018) [12], Ananiev et al. (1961) [42], and Marinheiro et al. (2023) [5]. The correlation of Cavallini et al. (2006) [11] has been reported to be accurate by these researchers as well as by many other researchers.

The correlations mentioned in the previous paragraph were considered for the calculation of h_{SAT}, which is to be determined at $x = 1$. The correlations of Shah and Cavallini et al. are indeterminate at $x = 1$. Hence, the calculations were carried out using $x = 0.999$ with all correlations.

The fluid properties were calculated with REFPROP 9.1, as in Lemmon et al. (2013) [38].

The results of the evaluation using various correlations for h_{SAT} are given in Table 5. The best agreement is with the Cavallini correlation with MAD of 22.0%. The next best is the Shah correlation, with a MAD of 22.3%. The results are discussed in Section 5.

Table 5. Deviations of Model 2 using various correlations for h_{SAT}.

Data of	Tube Type	Dia., mm	Fluid	Reduced Pressure	N	Deviation, % MAD (Upper Row)/AD (Lower Row) Using Correlation of					
						Shah (2022b) [10]	Cavallini et al. (2006) [11]	Dorao and Fernandino	Moradkhani et al.	Ananiev et al.	Marinheiro et al.
Lee et al. (1991) [21]	Plain	7.95	R-22	0.1763	1	7.8 −7.8	8.1 8.1	4.9 −4.9	14.3 14.3	6.4 −6.4	1.9 1.9
Fujii et al. (1978) [39]	Plain	21.4	R-113	0.0252 0.0323	15	15.1 −15.1	10.7 9.5	11.1 1.1	61.4 61.4	6.1 1.2	8.0 3.4
Kondou and Hrnjak (2011a, 2011b, 2012) [26,35,40]	Plain	6.1	CO_2	0.678 0.9492	35	19.1 −16.2	18.2 −5.2	23.5 13.5	13.3 −7.5	21.8 −4.7	19.0 7.5
Kondou and Hrnjak (2012) [26]	Plain	6.1	R-410A	0.5493 0.9468	37	27.4 −0.6	29.9 12.7	41.4 35.9	28.8 26.1	33.7 9.3	35.8 31.8
Agarwal and Hrnjak (2015) [29]	Plain	6.1	R-134a	0.3247	4	24.7 −15.7	19.1 −4.5	19.7 −5.6	18.8 4.9	25.7 −17.6	15.8 5.8
			R-1234ze	0.2743	5	26.5 16.5	30.0 24.1	28.2 20.5	38.3 38.3	26.3 15.8	31.7 28.7
			R-32	0.5433	6	25.6 −11.5	21.7 −3.8	20.3 8.4	20.3 8.5	24.5 −9.6	21.4 11.6
All data	Plain	6.1 21.4		0.0252 0.9492	103	22.3 −8.5	22.0 5.0	27.8 8.9	27.7 18.8	24.3 1.4	23.9 16.8

For Lee et al. data point, $G = 250$ kg/m^{2}s; superheat, 21.3 K.

4. Discussion

4.1. Discussion Saturated Condensation

4.1.1. Overall Accuracy of Correlations

The deviations of the correlations that were evaluated are listed in Tables 2 and 3. It can also be seen that for all data, the Shah (2022b) [10] correlation has the least MAD at 17.3%. The next best is the Shah (2009, 2013) [7,8] correlation, with a MAD of 20.3%. The correlations of Moradkhani et al., Marinheiro et al., and Dorao and Fernandino have MADs of 20.9%, 21.7%, and 21.9%, respectively. So, their overall performance is good. The MADs of Kim and Mudawar and Ananiev et al. correlations are 27.3% and 26.3%, respectively. The correlations of Moser et al., Nie et al., and Traviss et al. have MADs of 34.2%, 54.7%, and 98.5%, respectively; hence, these are very unreliable and not discussed any further.

In Shah (2022b) [10], it was shown that the Shah correlation was the most accurate among the correlations evaluated. The new correlations evaluated during the present research, Nie et al. and Marinheiro et al., have been found to be less accurate than the Shah correlation, as well as some other correlations.

4.1.2. Weber Number and the Mini-Macro Channel Boundary

According to the Shah (2022a, 2022b) [3,10] correlation, the Weber number only has an effect on the horizontal channels. In Table 2, it can be seen that the MADs of all

correlations except the Shah (2022b) [10] correlation increase drastically when $We_{GT} < 100$ in the horizontal channels. For example, the MAD of Marinheiro et al. correlation is 19.1% when $We_{GT} > 100$ and 31.6% when $We_{GT} < 100$. The Weber number is the ratio of the force of inertia to the force of surface tension. These results show that $We_{GT} = 100$ is the transition point between the regions in which surface tension has an effect and those in which surface tension does not have an effect. Thus, this is the boundary between mini and macro channels. Usually, D = 3 mm is considered to be the boundary between mini and macro channels. The results in Table 2 show that the data for D < 3 mm are in good agreement with the more accurate correlations if $We_{GT} > 100$. Hence, D = 3 mm does not represent the boundary between the presence or absence of the surface tension effect. This topic is discussed in detail in Shah (2018) [43] and Shah (2021) [2].

It is clear from the results in Table 2 that only the Shah (2022b) [10] correlation should be used for horizontal channels when $We_{GT} < 100$.

Figures 1 and 2 show the comparison of some data for low Weber numbers with some correlations.
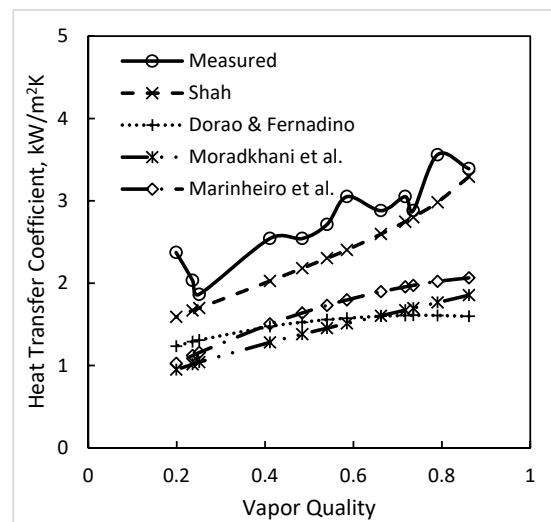
Figure 1. Comparison of the data of Bashar et al. (2018) [44] for saturated condensation with various correlations. R-134a in a horizontal tube: D = 2.14 mm; T_{SAT} = 30 °C; G = 50 kg/m^{2}s; and We_{GT} = 22.
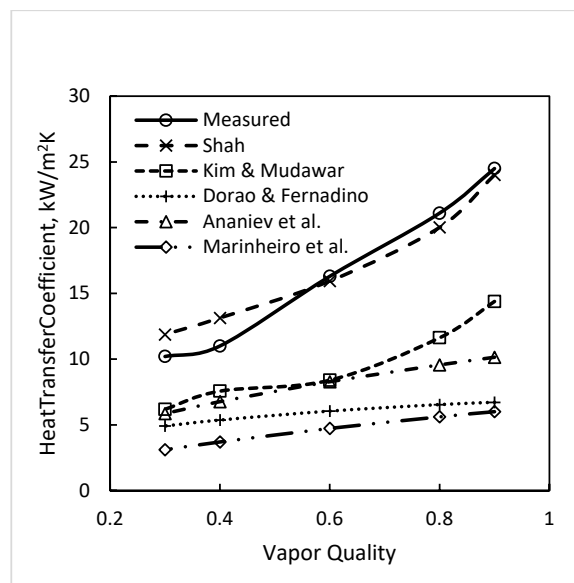
Figure 2. Comparison of correlations with data of Wang and Du (2000) [45] for water in a horizontal tube: D = 3.95 mm; T_{SAT} = 105 °C; G = 11.2 kg/m^{2}s; and We_{GT} = 12.

4.1.3. Effect of Flow Orientation

It can be seen in Table 2 that for vertical flow, the Shah correlations have a MAD of 17.4%, while the deviations of all other correlations are much higher. The next best is Moradkhani et al., with a MAD of 27.2%. The correlations of Marinheiro et al. and Nie et al. have MADs of 29.6% and 131.5%, respectively. Only the Shah correlations distinguish between the horizontal and vertical channels. The phenomena in the two orientations are different because flows in the horizontal channels are asymmetrical at lower flow rates due to the effect of gravity, while the flow is symmetrical under vertical flow. Only the Shah correlations take these effects into account and are, therefore, able to predict heat transfer correctly. Other correlations do not take these into consideration and, therefore, fail to predict correctly. Figures 3 and 4 show a comparison of some correlations with the data in the vertical tubes.
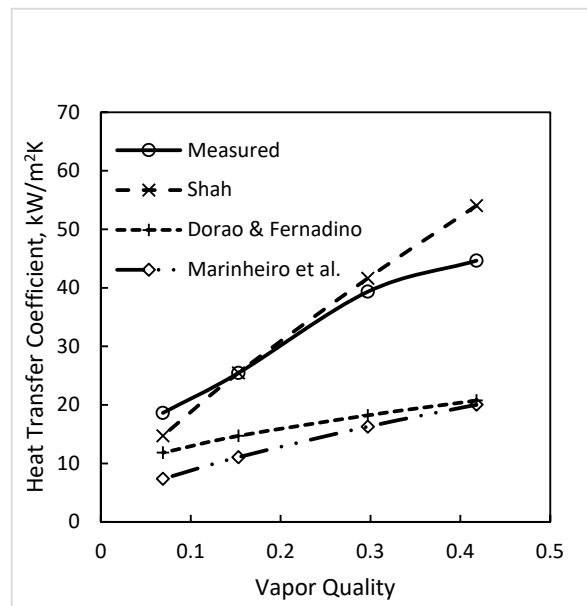
Figure 3. Data of Goodykoontz and Dorsch (1967) [46] for water in a vertical tube compared to correlations: D = 7.44 mm; T_{SAT} = 110 °C; and G = 265 kg/m^{2}s.
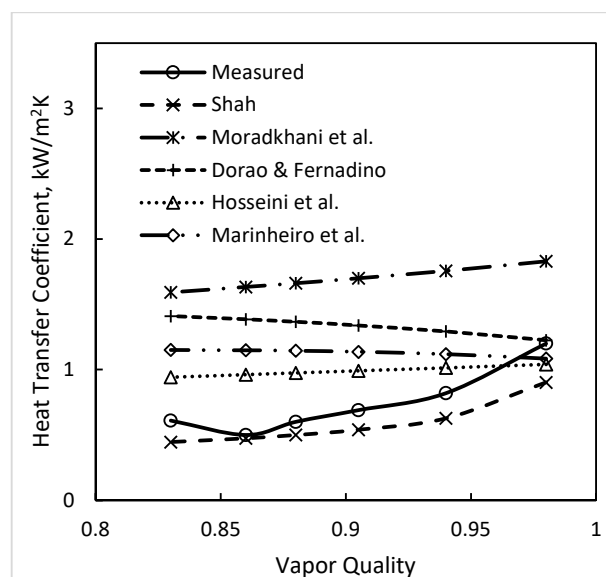
Figure 4. Data of Lilburne and Wood (1982) [47] for R-113 in a vertical tube compared to some correlations: D = 3.47 mm; T_{SAT} = 52 °C; and G = 50 kg/m^{2}s.

It may be concluded that only the Shah correlation is applicable to vertical channels without any limit. Other correlations can only be considered for high flow rates.

4.1.4. Type of Fluids

Table 3 lists the deviations in the correlations with various fluids and fluid types. The Shah (2022b) [10] correlation gives the best agreement with all fluids. So, only the other correlations are discussed.

For halocarbon refrigerants, several correlations are in good agreement with the data, the best among them being Marinheiro et al., Moradkahni et al., and Dorao and Fernandino. These three are also in fairly good agreement with the data for hydrocarbons and carbon dioxide. For water, all correlations have large deviations except for the Shah correlations. The main reason is that the properties of water are very different from those of other fluids, and most of the databases used for developing these correlations had little or no data for water. For example, the databases used by Marinheiro et al. and Moradkhani et al. had water data from only one source each. There were none for water in the databases of Dorao and Ferandino and Hosseini et al. Therefore, it is not surprising that their correlations do not agree with most of the data for water. The correlation of Ananiev et al. was based exclusively on their data for water. However, all their data were at higher pressures and higher flow rates and were only in vertical tubes. The present database includes low pressures and flow rates as well as both horizontal and vertical channels. That is why their correlation has large deviations when all data for water are considered. As was discussed in Shah (2022a) [3], there is a lack of accurate data for ammonia, but there are reasons to believe that the Shah correlations are applicable to ammonia.

The conclusion is that the Shah correlations are reliable for all fluids and are to be preferred over other correlations. The correlations of Marinheiro et al., Moradkahni et al., and Dorao and Fernandino can be considered for fluids other than water, keeping in mind the limitations noted in Sections 4.1.2 and 4.1.3.

4.2. Discussion on Superheated Condensation

4.2.1. Accuracy of Models

A comparison of the predictions of the three models evaluated is shown in Table 4 and Figures 5–7.
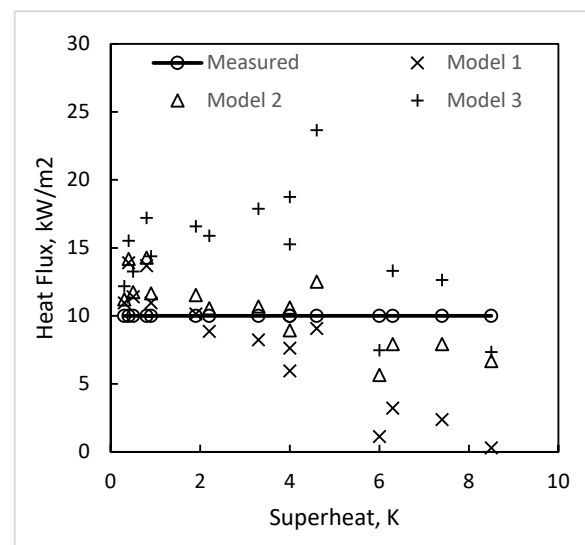
Figure 5. Comparison of predictions of models for superheated vapor condensation using the measured heat transfer coefficients. Data of Kondou and Hrnjak (2012a) [26] for CO_2: $p_r = 0.949$; $G = 150 \text{ kg/m}^2\text{s}$.
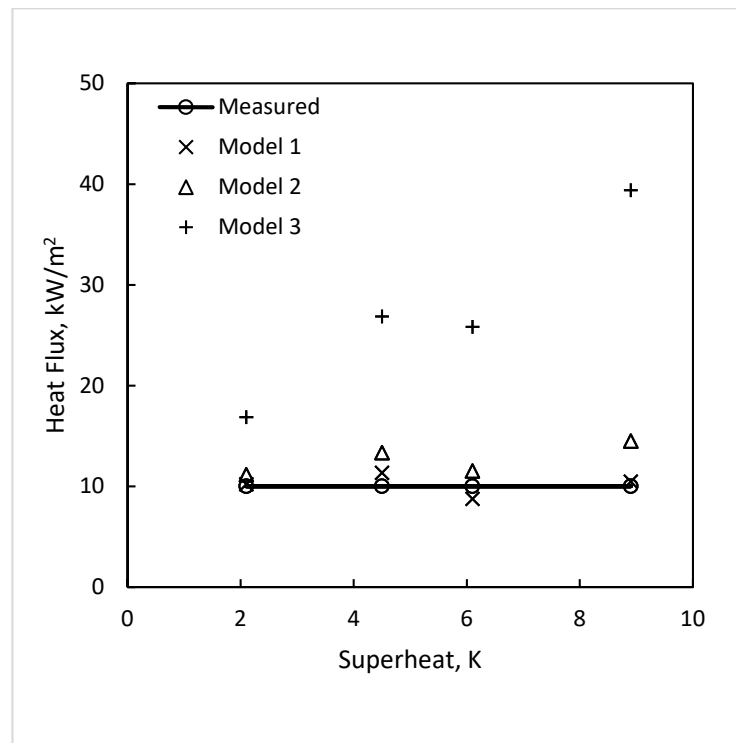
Figure 6. Comparison of the predictions of superheated condensation models using measured heat transfer coefficients. Data of Kondou and Hrnjak (2012a) [26] for R-410A: G = 100 kg/m²s; p$_r$ = 0.949.
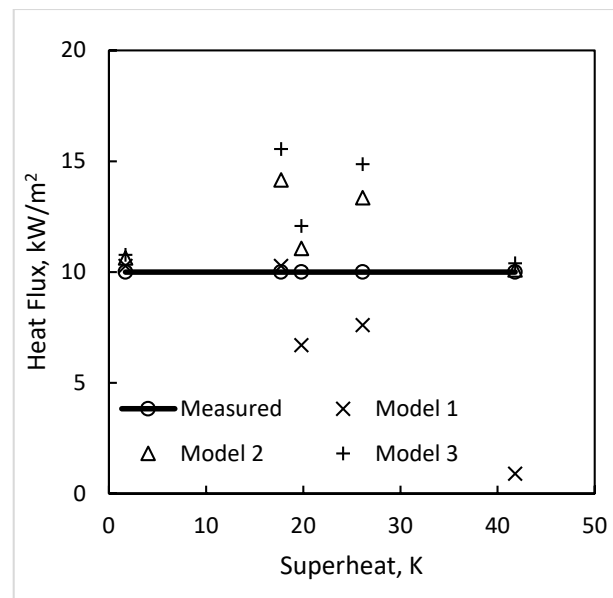
Figure 7. Comparison of the predictions of superheated condensation models using measured heat transfer coefficients. Data of Agarwal and Hrnjak (2015) [29] for R-1234 ze: G = 100 kg/m²s; T$_{SAT}$ = 50 °C.

Model 1, given by Equation (12), neglects the effect of superheating on the condensation heat transfer. As seen in Table 4, this model always underpredicts the local heat flux, with the AD for all data being −27.9%. Hence, for a condenser in which a large part of it is involved in superheated condensation, this model is not acceptable as it greatly underpredicts heat transfer. Its use may be justified in condensers where only a small part of it has superheated condensation.

Model 2, given by Equation (13), is seen to be, by far, the most accurate among the four models tested, with a MAD of 15.9%. On the other hand, Model 3, which was proposed by Webb (1998) [23], has a MAD of 33.4%. The two models differ only in terms of the mass transfer enhancement factor introduced by Webb. Webb proposed this model based on the idea that the single-phase heat transfer of superheated vapor is enhanced by mass transfer from the superheated vapor to the condensate film. He himself only compared this model with the data of Lee et al. (1991) [21], which were at a reduced pressure of 0.1763 and found good agreement. A study of the results of the data analysis showed that while Model 2 predicts higher than Model 2 in most cases, the difference becomes very high near the critical pressure. This is further evident in Figures 5–7. Close to critical pressure, Model 2 is seen to grossly overpredict the measured values. This may be attributed to the fact that the latent heat becomes very small near the critical pressure, resulting in the mass transfer effect factor in this model becoming very large.

Longo et al. (2015) [24] incorporated the Webb model (Model 3) into their procedure for calculating the mean heat transfer coefficient for plate-type heat exchangers. They reported good agreement with mean heat transfer coefficients for complete condensation of several fluids. However, it should be noted that the area over which superheated condensation occurs is only a small part of the total area of the heat exchanger. The highest reduced pressure in the data analyzed by Longo et al. was about 0.5, nowhere close to the range in which large deviations have been found in the present data analysis. Hence, good agreement of mean heat transfer coefficients reported by Longo et al. does not provide clear evidence of the accuracy of the Webb model.

The present data analysis indicates that the Webb model is less accurate than Model 2. However, the inaccuracy is not large at moderate pressure. At pressures close to critical, it grossly overpredicts and should not be used.

4.2.2. Choice of Correlations for Use in Model 2

For the calculation of the forced convection heat transfer coefficient of superheated vapor, two correlations were evaluated. These are the Dittus–Boelter equation, Equation (26), and the Gnielinski correlation with the Pethukov correction factor, which requires the insertion of wall temperature. The deviations were about the same using either of the two correlations. Hence, either of them can be used for the design.

As for the correlations for the condensing heat transfer coefficient, the least deviation was obtained with the Cavallini correlation, with its MAD being 22.0%. The next best was the Shah (2022b) [10] correlation, with a slightly higher MAD of 22.3%. Deviations using other correlations ranged from 23.9% to 27.8% and are thus significantly higher. Hence, the results suggest that the correlations of Shah and Cavallini et al. are preferable.

The correlation of Cavallini et al. requires inputting the wall temperature in their ΔT-dependent regime. As the wall temperature is unknown and is to be determined, iterative calculations are required that increase the calculation effort. On the other hand, the Shah correlation does not involve the insertion of the wall temperature as input; hence, calculations with it are simpler. It should also be noted that Cavallini et al. recommended their correlation only for $p_r \leq 0.8$.

As discussed in Section 4, the Shah correlation is the only one that is accurate at $We_{GT} < 100$; all other correlations that were evaluated have large deviations. Further, the Shah correlation is the only one that gives good agreement with the data for vertical channels.

In view of its simplicity and verified superior accuracy under all conditions, the Shah correlation appears to be the best choice for use in design. Other correlations may only be considered for horizontal channels with $We_{GT} > 100$ and within their limitations noted in Section 4.1.

Figures 8–10 show the comparison of the data with Model 2 using various correlations for h_{SAT}.
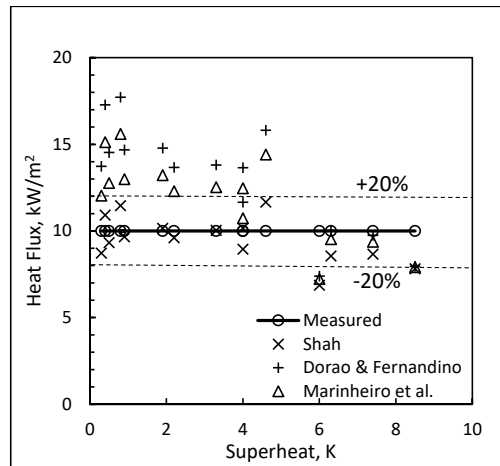
Figure 8. Comparison of the predictions of Model 2 using various correlations for h_{SAT}. Data of Kondou and Hrnjak (2022a) [26] for CO_2: p_r = 0.949; G = 150 kg/m^{2}s.
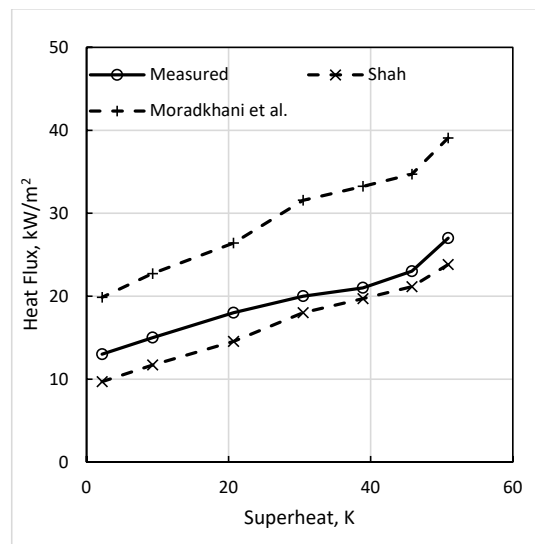
Figure 9. Evaluation of Model 2 with h_{SAT} using various correlations. Data of Fujii et al. (1978) [39] for R-113: G = 115 kg/m^{2}s; T_{SAT} = 50 $^\circ$C.
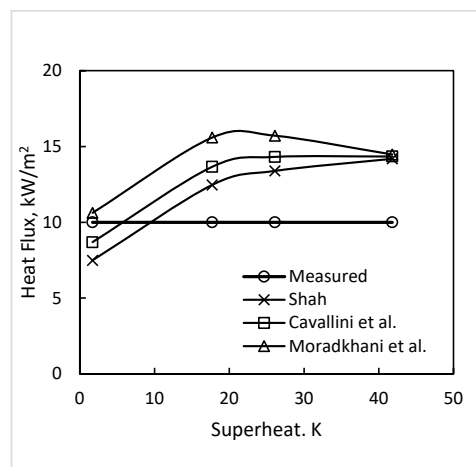
Figure 10. Evaluation of Model 2 with h_{SAT} using various correlations. R-1234ze at saturation temperature of 50 $^\circ$C, G = 100 kg/m^{2}s. Data of Agarwal and Hrnjak (2015) [29]. From Shah (2023) [1].

4.2.3. Application to Mixtures

The only data for the mixtures analyzed in the present research is for R-410A. As the glide of this fluid is very small, the results obtained do not shed light on the applicability to mixtures with significant glide. As was mentioned in Section 2.2, Jacob and Fronk (2021) [34] performed tests on the condensation of the superheated vapors of five mixtures with a glide up to 6.3 K. They analyzed the data using Equation (13) with h_{SAT} by the Cavallini et al. correlation and vapor forced convection heat transfer via the Gnielinski correlation. A correction was made for the mass transfer effect using the method of Bell and Ghaly. Good agreement with the data was found. Therefore, it can be concluded that Model 2 can be applied to mixtures with Bell–Ghaly correction, at least for glides up to 6.3 K.

5. Conclusions

1. Published correlations, including the two latest, for the condensation of saturated vapors in channels were compared to a very wide-ranging database. It included data for 51 pure fluids and mixtures from 132 sources in horizontal and vertical channels of many shapes. The hydraulic diameters of the channels were 0.08–49 mm, with a mass flux of 1.1–1400 kg/m^{2}s and reduced pressures of 0.0006–0.949. The fluids included water, CO_2, ammonia, hydrocarbons, halocarbon refrigerants, various chemicals, and heat transfer fluids.

2. The results showed that the Shah (2022b) [10] correlation has the best agreement with the saturated condensation data of all fluids and channel types/shapes under all conditions for both horizontal and vertical orientations. Other correlations have larger deviations, especially for water and vertical channels. All correlations other than the Shah (2022b) [10] correlation have large deviations in horizontal channels when $We_{GT} < 100$; this is the range in which surface tension has an effect. Further, all correlations other than those of Shah have large deviations from the data for vertical channels.

3. Three widely used models for condensation from superheated vapors were evaluated through comparison with test data, using measured heat transfer coefficients for saturated condensation and single-phase forced convection of superheated vapor. The models given by McAdams and Webb were found to underpredict and overpredict the data, respectively. The other model (Model 2), which obtains total heat flux by adding heat fluxes due to saturated condensation and single-phase forced convection, was found to be satisfactory.

4. Model 2 for superheated condensation was compared to the data using various correlations for saturated condensation and single-phase forced convection. For saturated condensation, the correlations of Shah and Cavallini et al. were found to have the best agreement. For the single-phase forced convection of vapor, the correlations of Gnielinski and Dittus–Boelter both yielded good results.

5. Model 2 can also be used for mixtures by applying the Bell and Ghaly correction for the mass transfer effect.

Data Availability Statement: All data used are from publicly available publications.

Conflicts of Interest: The author declares no conflict of interest.

Nomenclature

AD	Average deviation, (-)
C_{PG}	Specific heat of vapor at constant pressure, J kg^{-1}K^{-1}
D	Inside diameter of the tube, m
D_{HP}	Equivalent diameter = (4 X flow area)/(perimeter with heat transfer), m
D_{HYD}	Hydraulic equivalent diameter = (4 X flow area)/(wetted perimeter), m
Fr_{LT}	Froude number = $G^2\rho_L{}^{-2}g^{-1}D^{-1}$, (-)
f	Darcy friction factor for pipe flow, (-)

G	Total mass flux (liquid + vapor), kg m^{-2}s^{-1}
g	Acceleration due to gravity, m s^{-2}
h	Heat transfer coefficient, W m^{-2} K^{-1}
h$_{FC}$	Forced convection single-phase heat transfer coefficient of vapor, W m^{-2} K^{-1}
h$_{GS}$	Heat transfer coefficient assuming vapor phase flowing alone in the tube, Wm^{-2} K^{-1}
h$_{SAT}$	Heat transfer coefficient of saturated vapor at x = 1, W m^{-2} K^{-1}
h$_{TP}$	Two-phase heat transfer coefficient, W m^{-2} K^{-1}
i$_{LG}$	Latent heat of vaporization. kJ kg^{-1}
J$_g$	Dimensionless vapor velocity, (-)
k	Thermal conductivity, W m^{-1} K^{-1}
MAD	Mean absolute deviation, (-)
N	Number of data points, (-)
p$_r$	Reduced pressure, (-)
Pr	Prandtl number, (-)
q	Heat flux, Wm^{-2}
q$_{lat}$	Heat flux due to phase change only, Wm^{-2}
Re	Reynolds number = GDμ^{-1}, (-)
Re$_{GS}$	Superficial Reynolds number of vapor = GxDμ$_G$$^{-1}$, (-)
Re$_{GT}$	Reynolds number for all mass flowing as vapor = GDμ$_G$$^{-1}$, (-)
Re$_{LS}$	Superficial Reynolds number of liquid = G $(1-x)$Dμ$_L$$^{-1}$, (-)
T	Temperature, K
T$_{SAT}$	Saturation temperature, $^{\circ}$C
T$_w$	Wall temperature, $^{\circ}$C
ΔT	$= (T_{SAT} - T_w)$, K
We$_{GT}$	Weber number for all mass flowing as vapor, (-)
X$_{tt}$	Martinelli parameter = $\left(\frac{1}{x}-1\right)\left(\frac{\rho_G}{\rho_L}\right)^{0.5}\left(\frac{\mu_L}{\mu_G}\right)^{0.1}$, (-)
x	Vapor quality, (-)
Greek	
μ	Dynamic viscosity, Pa. s
ρ	Density, kg m^{-3}
Σ	Mathematical symbol for summation
σ	Surface tension, Nm^{-1}
Subscripts	
G	Vapor
L	Liquid
m	Mean
TP	Two-phase
w	Wall

References

1. Shah, M.M. Prediction of heat transfer during condensation of superheated vapor flowing inside channels. In Proceedings of the ASME IMECE Conference, New Orleans, LA, USA, 29 October–2 November 2023. Paper IMECE2023-110451.
2. Shah, M.M. *Two-Phase Heat Transfer*; John Wiley & Sons: Hoboken, NJ, USA, 2021.
3. Shah, M.M. Improved correlation for heat transfer during condensation in mini and macrochannels. *Int. J. Heat Mass Transf.* **2022**, *194*, 123069. [CrossRef]
4. Nie, F.; Wang, H.; Zhao, Y.; Song, Q.; Yan, S.; Gong, M. A universal correlation for flow condensation heat transfer in horizontal tubes based on machine learning. *Int. J. Therm. Sci.* **2023**, *184*, 107994. [CrossRef]
5. Marinheiro, M.M.; Marchetto, D.B.; Furlan, G.; de Souza Netto, A.T.; Tibiriçá, C.B. A robust and simple correlation for internal flow condensation. *Appl. Therm. Eng.* **2024**, *236*, 121811. [CrossRef]
6. Shah, M.M. A general correlation for heat transfer during film condensation inside pipes. *Int. J. Heat Mass Transf.* **1979**, *22*, 547–556. [CrossRef]
7. Shah, M.M. An improved and extended general correlation for heat transfer during condensation in plain tubes. *HVACR Res.* **2009**, *15*, 889–913. [CrossRef]
8. Shah, M.M. General correlation for heat transfer during condensation in plain tubes: Further development and verification. *ASHRAE Trans.* **2013**, *119*, 3–11.
9. Shah, M.M. A new correlation for heat transfer during condensation in horizontal mini/micro channels. *Int. J. Refrig.* **2016**, *64*, 187–202. [CrossRef]
10. Shah, M.M. Improved general correlation for condensation in channels. *Inventions* **2022**, *7*, 114. [CrossRef]

11. Cavallini, A.; Del Col, D.; Doretti, L.; Matkovic, M.; Rossetto, L.; Zilio, C. Condensation in horizontal smooth tubes: A new heat transfer model for heat exchanger design. *Heat Transf. Eng.* **2006**, *27*, 31–38. [CrossRef]

12. Dorao, C.A.; Fernandino, M. Simple and general correlation for heat trans- fer during flow condensation inside plain pipes. *Int. J. Heat Mass Transf.* **2018**, *122*, 290–305. [CrossRef]

13. Hosseini, S.H.; Moradkhani, M.A.; Valizadeh, M.; Zendehboudi, A.; Olazar, M. A general heat transfer correlation for flow condensation in single port mini and macro channels using genetic programming. *Int. J. Refrig.* **2020**, *119*, 376–389. [CrossRef]

14. Moradkhani, M.A.; Hosseini, S.H.; Song, M. Robust and general predictive models for condensation heat transfer inside conventional and mini/micro channel heat exchangers. *Appl. Therm. Eng.* **2022**, *201 Pt A*, 117737. [CrossRef]

15. Kim, S.; Mudawar, I. Universal approach to predicting heat transfer coefficient for condensing mini/micro-channel flow. *Int. J. Heat Mass Transf.* **2013**, *56*, 238–250. [CrossRef]

16. Bell, K.; Ghaly, M. An approximate generalized design method for multicomponent/partial condenser. *Am. Inst. Chem. Eng. Symp. Ser.* **1973**, *69*, 72–79.

17. McAdams, W.H. *Heat Transmission*, 3rd ed.; McGraw Hill: New York, NY, USA, 1954.

18. Merkel, F. *Die Grundlagen der Warmeubertragung*; T. Steinkopf: Leipzig, Germany, 1927; Quoted in McAdams (1954).

19. Altman, M.; Staub, F.W.; Norris, R.H. Local heat transfer and pressure drop for refrigerant-22 condensing in horizontal tubes. *Chem. Eng. Progr. Symp. Ser.* **1959**, *56*, 151–159.

20. Miropolsky, Z.l.; Shneersva, R.I.; Teernakova, L.M. Heat transfer at superheated steam condensation inside tubes. In Proceedings of the 5th International Heat Transfer Conference, Tokyo, Japan, 3–7 September 1974; Volume 3, pp. 246–249.

21. Lee, C.C.; Teng, Y.J.; Lu, D.C. Investigation of condensation heat transfer of superheated R-22 vapor in a horizontal tube. In *Proceedings of the World Conference on Experimental Heat Transfer of Fluid Mechanics and Thermodynamics, Dubrovnik, Yugoslavia, 23–28 June 1991*; Keffer, J.F., Shah, R.K., Ganić, E.N., Eds.; Elsevier: Amsterdam, The Netherlands, 1991; pp. 1051–1057.

22. Gnielinski, V. New equation of heat and mass transfer in turbulent pipe and channel flow. *Int. Chem. Eng.* **1976**, *16*, 359–367.

23. Webb, R.L. Convective condensation of superheated vapor. *ASME J. Heat Transf.* **1998**, *120*, 418–421. [CrossRef]

24. Longo, G.A.; Righetti, G.; Claudio Zilio, C. A new computational procedure for refrigerant condensation inside herringbone-type Brazed Plate Heat Exchangers. *Int. J. Heat Mass Transf.* **2015**, *82*, 530–536. [CrossRef]

25. Karwacki, J.; Butrymowicz, D.; Smierciew, E.; Przybylinski, T. Experimental investigations of condensation of superheated vapor in tube. In Proceedings of the 23rd IIR International Congress Refrigeration, Prague, Czech Republic, 21–26 August 2011. paper ID. 697.

26. Kondou, C.; Hrnjak, P.S. Condensation from superheated vapor flow of R744 and R410A at subcritical pressures in a horizontal smooth tube. *Int. J. Heat Mass Transf.* **2012**, *55*, 2779–2791. [CrossRef]

27. Petukhov, B.S. *Heat Transfer and Friction in Turbulent Pipe Flow with Variable Physical Properties*; Elsevier: Amsterdam, The Netherlands, 1970; Volume 6.

28. Agarwal, R.; Hrnjak, P.S. Effect of sensible heat, condensation in superheated and subcooled region incorporated in unified model for heat rejection in condensers in horizontal round smooth tubes. *Appl. Therm. Eng.* **2014**, *71*, 378–388. [CrossRef]

29. Agarwal, R.; Hrnjak, P.S. Condensation in two phase and desuperheating zone for R1234ze(E), R134a and R32 in horizontal smooth tubes. *Int. J. Refrig.* **2015**, *50*, 172–183. [CrossRef]

30. Xiao, J.; Hrnjak, P. Heat transfer and pressure drop of condensation from superheated vapor to subcooled liquid. *Int. J. Heat Mass Transf.* **2016**, *103*, 1327–1334. [CrossRef]

31. Xiao, J.; Hrnjak, P. A heat transfer model for condensation accounting for non-equilibrium effects. *Int. J. Heat Mass Transf.* **2017**, *111*, 201–210. [CrossRef]

32. Xiao, J.; Hrnjak, P. Flow regime map for condensation from superheated vapor. In Proceedings of the International Refrigeration and Air Conditioning Conference, Aqaba, Jordan, 8–10 March 2015; Paper 1910. Available online: https://docs.lib.purdue.edu/iracc/1910 (accessed on 16 December 2023).

33. Sieres, J.; Martín, E.; Martínez-Suárez, J.A. Condensation of superheated R134a and R437A inside a vertical tube. *Sci. Technol. Built Environ.* **2017**, *23*, 884–895. [CrossRef]

34. Jacob, T.A.; Fronk, B.M. A heat transfer model to predict superheated and saturated condensation of HFC/HFO refrigerant mixtures. *Int. J. Heat Mass Transf.* **2021**, *170*, 120947. [CrossRef]

35. Kondou, C.; Hrnjak, P.S. Effect of microfins on heat rejection in desuperheating, condensation in superheated region and two-phase zone. In Proceedings of the International Refrigeration and Air Conditioning Conference, Purdue, IN, USA, 16–19 July 2012; Paper 1345. Available online: https://docs.lib.purdue.edu/iracc/1345 (accessed on 16 December 2023).

36. Blangetti, F.; Schlunder, E.U. Local heat transfer coefficients in film condensation at high Prandtl numbers. In *Condensation Heat Transfer*; Marto, P.J., Kroger, P.G., Eds.; American Society of Mechanical Engineers: New York, NY, USA, 1979; pp. 17–25.

37. Vinš, V.; Aminian, A.; Celný, D.; Součková, M.; Klomfar, J.; Čenský, M.; Prokopová, O. Surface tension and density of dielectric heat transfer fluids of HFE type-experimental data at 0.1 MPa and modeling with PC-SAFT equation of state and density gradient theory. *Int. J. Refrig.* **2021**, *131*, 956–969. [CrossRef]

38. Lemmon, E.W.; Huber, L.; McLinden, M.O. *NIST Reference Fluid Thermodynamic and Transport Properties*; REFPROP Version 9.1; NIST: Gaithersburg, MD, USA, 2013.

39. Fujii, T.; Honda, H.; Nozu, S.; Nakarai, S. Condensation of superheated vapor inside a horizontal tube. *Heat Transf. Jpn. Res.* **1978**, *4*, 1–48.

40. Kondou, C.; Hrnjak, P.S. Heat rejection from R744 flow under uniform temperature cooling in a horizontal smooth tube around the critical point. *Int. J. Refrig.* **2011**, *34*, 719–731. [CrossRef]

41. Dittus, F.W.; Boelter, L.M.K. Heat transfer in automobile radiators of the tubular type. *Univ. Calif. Publ. Engl.* **1930**, *2*, 443–461, Reprinted in *Int. Commun. Heat Mass Transf.* **1985**, *12*, 3–22. [CrossRef]

42. Ananiev, E.P.; Boyko, I.D.; Kruzhilin, G.N. Heat transfer in the presence of steam condensation in horizontal tubes. *Int. Dev. Heat Transf.* **1961**, *2*, 290–295.

43. Shah, M.M. Applicability of correlations for boiling/condensing in macrochannels to minichannels. *Heat Mass Transf. Res. J.* **2018**, *2*, 20–32.

44. Bashar, M.K.; Nakamura, K.; Kariya, K.; Miyara, A. Experimental study of con-densation heat transfer and pressure drop inside a small diameter microfin and smooth tube at low mass flux condition. *Appl. Sci.* **2018**, *8*, 2146. [CrossRef]

45. Wang, B.X.; Du, X.Z. Study on laminar film-wise condensation for vapor flow in an inclined small/mini-diameter tube. *Int. J. Heat Mass Transf.* **2000**, *43*, 1859–1868. [CrossRef]

46. Goodykoontz, J.H.; Dorsch, R.G. *Local Heat Transfer Coefficients for Condensation of Steam in Vertical Downflow within a 5/8 Inch Diameter Tube*; NASA TN D-3326; National Aeronautics and Space Administration: Washington, DC, USA, 1967.

47. Lilburne, G.M.; Wood, D.G. Condensation inside a vertical tube. In Proceedings of the Seventh International Heat Transfer Conference, Munich, Germany, 6–10 September 1982; pp. 113–117.